COMPRESSIBILITY EFFECTS DUE TO PRESSURE FLUCTUATIONS IN HOMOGENEOUS SHEAR FLOW

Fujihiro Hamba
Institute of Industrial Science, University of Tokyo
Roppongi, Minato-ku, Tokyo 106-8558, Japan

ABSTRACT

Direct numerical simulation results are used to study compressibility effects on turbulent energy growth in homogeneous shear flow. Normalized amplitude of the pressure fluctuations is shown to decrease as the turbulent Mach number increases. This decrease causes the reduction in the pressure–strain term, changes the anisotropy of the Reynolds stress, and reduces the growth rate of turbulent kinetic energy as is the case of mixing layers. The transport equation for the pressure variance is examined in detail. It is shown that when the turbulent Mach number is high the pressure-variance dissipation term is not negligible and contributes to the reduction in the pressure fluctuations. The pressure-variance dissipation is closely related to the high-wavenumber part of the pressure-variance spectrum. Profile of the spectrum is observed to depend on the turbulent Mach number. A statistical theory is applied to obtain model expressions for the pressure-variance dissipation and the pressure–dilatation correlation.

INTRODUCTION

It is known that compressibility effects on turbulence in high-speed boundary layers and channel flows are due to the mean density and temperature variations (Lele 1994, Bradshaw 1996). Mean velocity profile can be derived from the Van Driest transformation of that in incompressible turbulence. Effects of the density and pressure fluctuations are very small. On the other hand, significant compressibility effects on turbulence are observed in high-speed mixing layers; the growth rate of thickness decreases as the Mach number increases. Similarly, the growth rate of turbulent kinetic energy in homogeneous shear flows is reduced as the turbulent Mach number increases. These reductions cannot be explained by the mean density variations; it is closely related to the density and pressure fluctuations.

Sarkar (1995) performed a direct numerical simulation (DNS) of homogeneous shear flow. He showed that the reduced growth rate of turbulent kinetic energy is not due to explicit dilatational effects but primary due to the reduced level of turbulence production; that is, the anisotropy of the Reynolds stress is changed due to compressibility effects. Vreman *et al.* (1996) used DNS to study the reduction in the growth rate of mixing layers. They showed that reduced pressure fluctuations are responsible for the change in growth rate via the pressure–strain term. Their results suggest that the behavior of the pressure fluctuations needs to be studied further to better understand compressibility effects.

Yoshizawa (1992, 1995, 1998) used a statistical theory called the two-scale direct-interaction approximation (TSDIA) to derive compressible turbulence models. He pointed out that compressibility effects are tightly linked with the density fluctuations and proposed a three-equation model that consists of the transport equations for the turbulent kinetic energy, its dissipation rate, and the density variance. However, Bradshaw (1996) pointed out that the density variance is not necessarily a good descriptor of compressibility effects. DNS of compressible channel flows with non-adiabatic walls showed that the density fluctuations can exist with little compressibility effects (Coleman *et al.* 1995, Huang *et al.* 1995). This is because the density fluctuations consist of the acoustic and entropy modes in general and the latter mode is dominant in channel flows. We cannot distinguish the two modes using the density variance only. Recently, using the TSDIA Rubinstein and Erlebacher (1997) derived transport coefficients in weakly

compressible turbulence. Instead of the density they adopted the pressure and the entropy as primary variables to clearly distinguish acoustic and entropy-related effects.

In this work, paying attention to the role of the pressure fluctuations we investigate compressibility effects in homogeneous shear flow. Following Hamba (1999) we study the reduction in the growth rate of turbulent kinetic energy using DNS data. We examine the transport equation for the pressure variance to understand the mechanism of reduced pressure fluctuations. We also apply the TSDIA to obtain model expressions for the pressure-variance dissipation and the pressure–dilatation correlation. To improve the analysis by Hamba (1999) we take an ensemble average to obtain better statistical quantities, examine the decomposition of the pressure–strain term in detail, and modify the model for the pressure-variance dissipation.

DNS RESULTS

The present simulation was performed in a 128^3 spatial grid in a cube of 2π using the spectral and third-order Runge-Kutta methods. Physical quantities are normalized by the mean density $\bar{\rho}$ and the mean speed of sound $\bar{c}$ where the mean is defined as a volume average over the computational domain. The mean velocity is $U_1=Sx_2$ where S is a constant shear rate. Initial velocity fluctuations are solenoidal; initial pressure fluctuations are calculated from the incompressible Poisson equation (see Hamba (1999) for details). The initial values of the microscale Reynolds number and the nondimensional shear rate were set to $R_\lambda=24$ and $SK/\varepsilon=7.1$, respectively. We investigate two cases in which the initial turbulent Mach number were set to $M_t=0.1$ and 0.3, respectively. For each case we perform five runs with different random numbers for the initial velocity fluctuations. We average results from five runs to obtain better statistical quantities.

It is well known that the growth rate of turbulent kinetic energy K is reduced due to compressibility effects (Sarkar 1995). In the present simulation the growth rate in the case of $M_t=0.3$ decreases by 30% compared to the case of $M_t=0.1$. Sarkar (1995) showed that the reduction in growth rate is primarily due to the reduced level of turbulence production. The production rate is proportional to the Reynolds shear stress $\langle u'_1u'_2\rangle$ because the shear rate S is constant. To clarify the reasons for the reduced shear stress we examine its transport equation normalized by SK:

$$\frac{1}{SK}\frac{d}{dt}\langle u'_1u'_2\rangle = -\frac{\langle u'^2_2\rangle}{K} - \frac{\varepsilon_{12}}{SK} + \frac{1}{SK\bar{\rho}}\Pi_{12} \qquad (1)$$

where ε_{12} and Π_{12} are the (1,2) components of the dissipation and pressure–strain tensors defined as

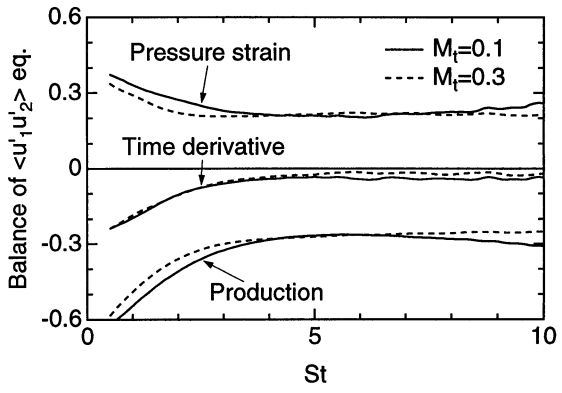

Figure 1. Time history of terms in the $\langle u'_1u'_2\rangle$ equation.

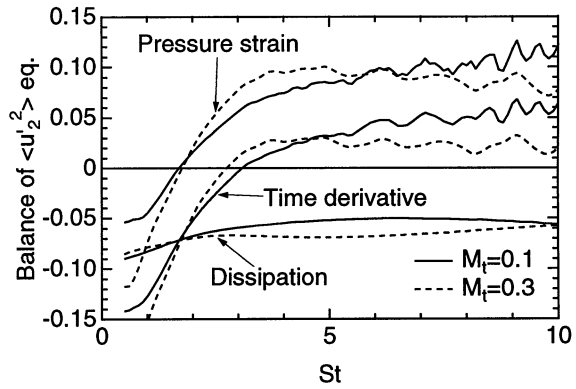

Figure 2. Time history of terms in the $\langle u'^2_2\rangle$ equation.

$$\varepsilon_{ij} = 2\bar{\nu}\left\langle \frac{\partial u'_i}{\partial x_k}\frac{\partial u'_j}{\partial x_k}\right\rangle, \quad \Pi_{ij} = \left\langle p'\left(\frac{\partial u'_i}{\partial x_j} + \frac{\partial u'_j}{\partial x_i}\right)\right\rangle \qquad (2)$$

respectively. Figure 1 shows the time history of the terms in the $\langle u'_1u'_2\rangle$ equation for $M_t=0.1$ and 0.3. Here and hereafter, the quantities whose time history is plotted are averaged from $t-\Delta t/2$ till $t+\Delta t/2$ where $\Delta t=0.12K_0/\varepsilon_0$ so that the trend of temporal evolution is emphasized by the reduction of oscillations. Since the viscous dissipation term ε_{12} is very small it is not plotted; the other three terms are shown in the figure. Since the shear stress is negative, a negative time-derivative term means a positive growth rate; it is slightly smaller for $M_t=0.3$ than for $M_t=0.1$. Both the production and pressure–strain terms decrease their amplitude as M_t increases. Since the pressure–strain term is positive its reduction acts as a gain in the shear-stress amplitude. Therefore, the decrease in shear-stress growth rate is due to the reduced level of the production term $-\langle u'^2_2\rangle/K$.

Then, we examine the transport equation for $\langle u'^2_2\rangle$:

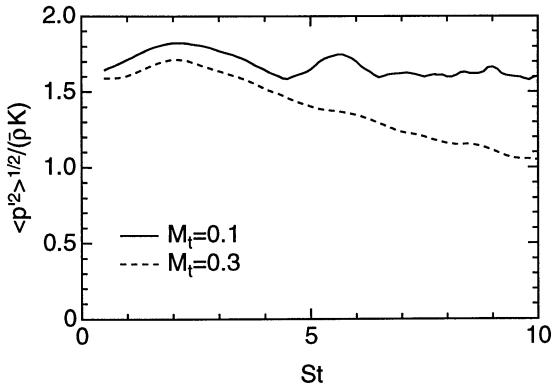

Figure 3. Time history of r.m.s. of the pressure fluctuation.

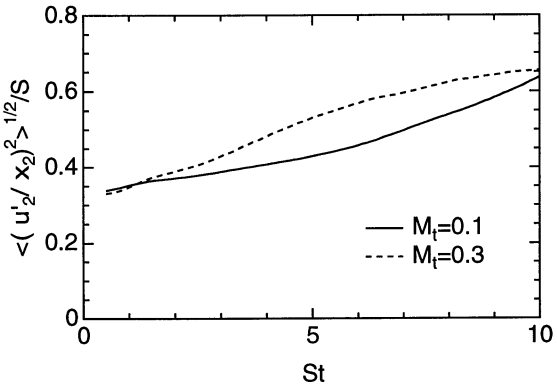

Figure 4. Time history of r.m.s. of the velocity gradient.

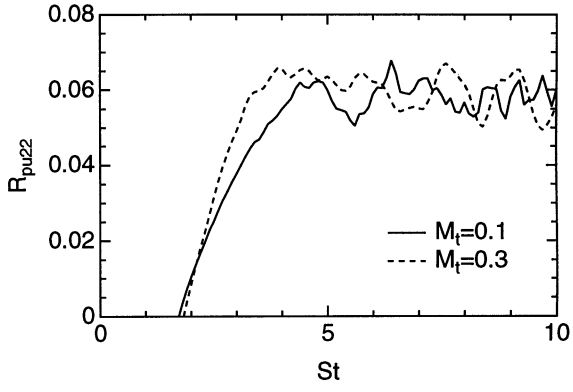

Figure 5. Time history of the correlation R_{pu22}.

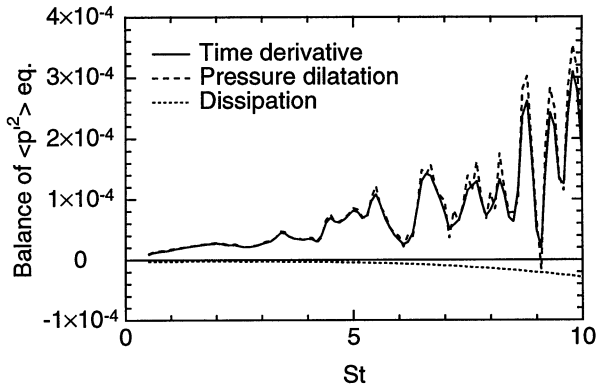

Figure 6. Time history of terms in the pressure-variance equation for M_t=0.1

$$\frac{1}{SK}\frac{d}{dt}\langle u_2'^2\rangle = -\frac{\varepsilon_{22}}{SK} + \frac{1}{SK\bar{\rho}}\Pi_{22} \qquad (3)$$

Figures 2 shows the time history of the terms in the above equations for M_t=0.1 and 0.3. It is clearly seen in Fig. 2 that the primary reason for the decrease in $\langle u'_2{}^2\rangle$ is the reduced level of the pressure–strain term Π_{22}. Therefore, it is necessary to investigate compressibility effects on the pressure–strain term to understand the mechanism of the reduction in turbulent energy growth rate.

Although we should examine the transport equation for the pressure–strain term as a next step, the equation is too much complicated compared to that for the turbulent energy component. Instead, we examine the pressure–strain term by decomposing it into three parts: the r.m.s. pressure fluctuation $\langle p'^2\rangle^{1/2}$, the r.m.s. velocity gradient $\langle(\partial u'_2/\partial x_2)^2\rangle^{1/2}$, and the correlation coefficient $R_{pu22}=\Pi_{22}/[\langle p'^2\rangle^{1/2}\langle(\partial u'_2/\partial x_2)^2\rangle^{1/2}]$. Figure 3 shows the time history of the r.m.s. pressure fluctuation $\langle p'^2\rangle^{1/2}$ normalized by $\bar{\rho}K$ for M_t=0.1 and 0.3. The fluctuation for M_t=0.3 decreases as time goes by whereas that for M_t=0.1 keeps nearly constant value in the average. Figure 4 shows the r.m.s. velocity gradient for M_t=0.1 and 0.3. This quantity is greater for M_t=0.3 than for M_t=0.1. Figure 5 shows the correlation R_{pu22} for M_t=0.1 and 0.3. The correlation is nearly the same for the two cases. Therefore, the reduced pressure fluctuations are the reason for the decrease in the pressure–strain term.

To clarify the mechanism of reduced pressure fluctuations in the homogeneous shear flow we examine the transport equation for the pressure variance. For homogenous shear flow the transport equation can be written as

$$\frac{d}{dt}\langle p'^2\rangle = -\varepsilon_p - 2\gamma P\langle p'd'\rangle + \text{Res.} \qquad (4)$$

where $d'=\nabla\cdot\mathbf{u}'$ and Res. denotes residual terms whose values are negligible compared to the main three terms. The pressure-variance dissipation ε_p is defined as

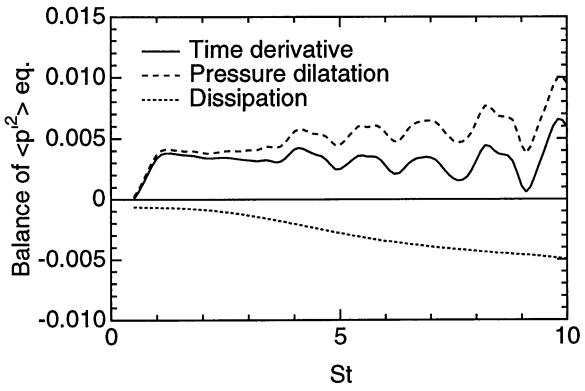

Figure 7. Time history of terms in the pressure-variance equation for M_t=0.3

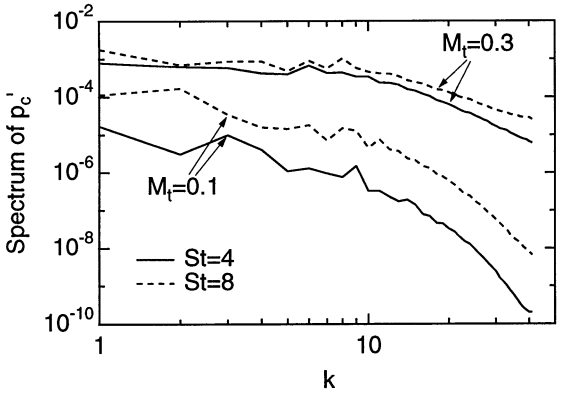

Figure 8. Spectrum of the variance of the compressible velocity pressure component at St=4 and 8.

$$\varepsilon_p = 2(\gamma-1)\bar{\lambda}\left\langle \frac{\partial p'}{\partial x_i}\frac{\partial \theta'}{\partial x_i}\right\rangle \qquad (5)$$

Figures 6 and 7 show the time history of the three terms in (4) for M_t=0.1 and 0.3, respectively. In Fig. 6 the dissipation term ε_p is small compared to the pressure dilatation; the temporal evolution of the pressure variance is determined solely by the pressure dilatation. On the other hand, in Fig. 7 the absolute value of ε_p is comparable to the pressure dilatation. In addition, the growth rate of pressure dilatation is reduced for M_t=0.3 compared to the case of M_t=0.1. Therefore, large value of the dissipation ε_p as well as reduced growth rate of pressure dilatation are the reasons for the reduced pressure fluctuations for M_t=0.3.

Here, we focus on the pressure-variance dissipation ε_p. Using a statistical analysis we can estimate the dissipation as follows:

$$\varepsilon_p \cong 2(\gamma-1)\bar{\kappa}\left\langle \frac{\partial p'}{\partial x_i}\frac{\partial p'}{\partial x_i}\right\rangle = 2(\gamma-1)\frac{\bar{\nu}}{P_r}\int_0^\infty dk\, k^2 E_p(k) \qquad (6)$$

where $P_r(=\bar{\nu}/\bar{\kappa})$ is the Prandtl number and $E_p(k)$ is the three-dimensional spectrum of the pressure variance. We divide p' into the incompressible part p'_s and the compressible part p'_c and assume each spectrum in the inertial range as

$$E_p(k) = E_{ps}(k) + E_{pc}(k) \qquad (7)$$

where

$$E_{ps}(k) \propto k^{-7/3} \qquad (8)$$

$$E_{pc}(k) \cong \bar{\rho}^2\bar{c}^2 E_c(k) \propto k^{-5/3-\alpha} \qquad (9)$$

In (8) Batchelor's spectrum is adopted for the spectrum of the incompressible component. In (9) the spectrum of the compressible component is assumed to be proportional to the compressible energy spectrum $E_c(k)$; parameter α denotes the deviation from the Kolmogorov spectrum. The relation $E_{pc}(k)=\bar{\rho}^2\,\bar{c}^2 E_c(k)$ means a balance between the acoustic potential and kinetic energies for dilatational fluid motions. Since the integrand in (6) contains k^2, the high-wavenumber part of $E_p(k)$ can contribute to the integral. Substituting (7)–(9) into (6) and integrating up to the Kolmogorov wavenumber $k_d(=\varepsilon^{1/4}\nu^{-3/4})$ we find that the contribution of $E_{ps}(k)$ to ε_p is of $O(\nu^{1/2})$; it is negligibly small at high Reynolds numbers. The contribution of $E_{pc}(k)$ to ε_p depends on α; if α= 0 then ε_p is of O(1) whereas if α>2/3 then $E_{pc}(k)<E_{ps}(k)$ and ε_p is of $O(\nu^{1/2})$.

Figure 8 shows the spectrum $E_{pc}(k)$ at St = 4 and 8 for M_t=0.1 and 0.3. Although the power of the spectral forms cannot be evaluated from these profiles due to low Reynolds numbers, we can see a qualitative difference between M_t=0.1 and 0.3. The spectrum $E_{pc}(k)$ rapidly decays as k increases for M_t=0.1; the profile corresponds to large value of α that causes small value of ε_p. On the other hand, the high-wavenumber part of $E_{pc}(k)$ for M_t=0.3 keeps relatively large values that contribute to ε_p.

The high-wavenumber part of $E_c(k)$ is similar to the corresponding spectrum $E_{pc}(k)$ (not shown). This means that the potential and kinetic energies almost balance at high wavenumbers. Using the eddy-damped quasi-normal Markovian (EDQNM) theory Bataille and Bertoglio (1993) showed that the compressible energy spectrum $E_c(k)$ is proportional to $k^{-11/3}$ if M_t is not very high whereas it tends to the Kolmogorov spectrum $k^{-5/3}$ as M_t increases to 1. Their results mean that α decreases from 2 to 0 as M_t increases. Such dependence of the spectrum $E_c(k)$ on M_t can explain the difference in $E_{pc}(k)$ between the cases of M_t=0.1 and 0.3.

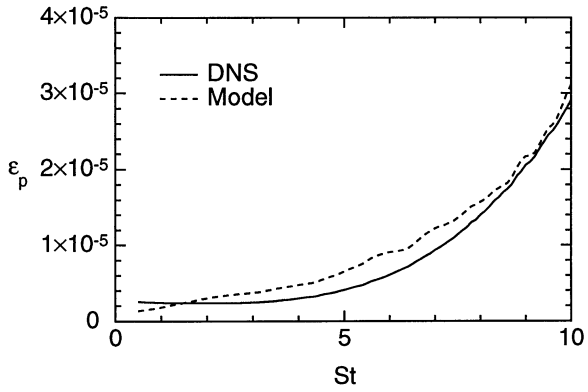

Figure 9. Time history of the pressure-variance dissipation for M_t=0.1.

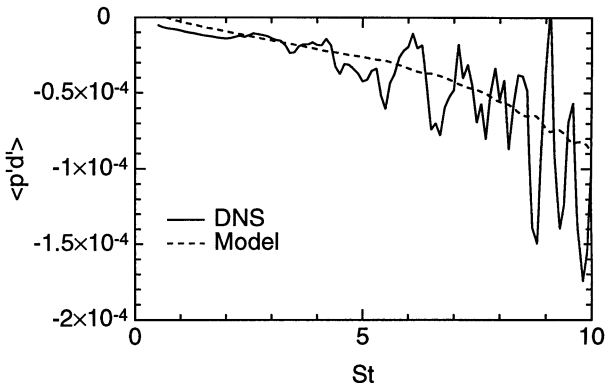

Figure 11. Time history of the pressure–dilatation correlation for M_t=0.1.

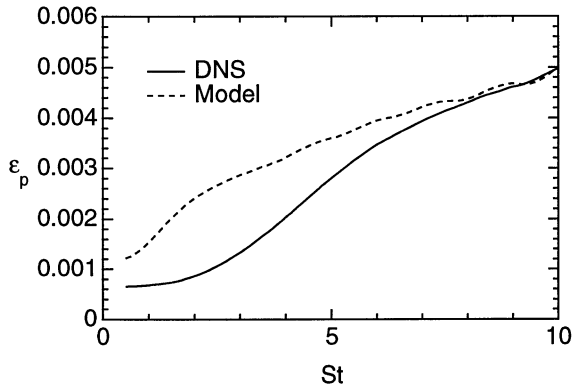

Figure 10. Time history of the pressure-variance dissipation for M_t=0.3.

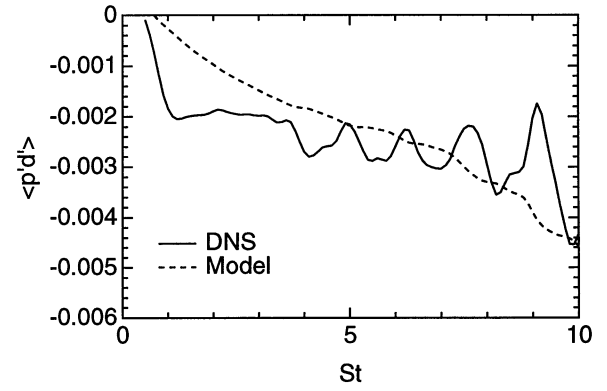

Figure 12. Time history of the pressure–dilatation correlation for M_t=0.3.

TURBULENCE MODELING

Here, we make an attempt to model pressure-related terms using the TSDIA. The procedure of TSDIA analysis is explained in Hamba and Blaisdell (1997) and Hamba (1999). First, we investigate the pressure-variance dissipation ε_p. The model expression for ε_p can be given by

$$\varepsilon_p = \begin{cases} C_{\varepsilon p1}\dfrac{\gamma-1}{P_r}\dfrac{\varepsilon\langle p'^2\rangle}{K} & \text{for } M_t \geq M_{t0} \\ C_{\varepsilon p1}\dfrac{\gamma-1}{P_r}\dfrac{\varepsilon\langle p'^2\rangle}{K} R_{e\tau}^{(M_t/M_{t0}-1)/2} & \text{for } 0 < M_t < M_{t0} \end{cases} \tag{10}$$

where $C_{\varepsilon p1}$ and M_{t0} are nondimensional model constants and $R_{e\tau}=K^2/(\varepsilon\nu)$. The factor $(\gamma-1)/P_r$ in (10) is originally included in the definition for ε_p. The part $C_{\varepsilon p1}(\varepsilon/K)\langle p'^2\rangle$ has the same expression as that for the scalar-variance dissipation in incompressible turbulence. The part of $R_{e\tau}$ is added by considering the dependence on ν as was discussed in the previous section. If M_t is high and α=0 in (9) then ε_p does not depend on ν; if M_t is low and $E_{ps}(k)>E_{pc}(k)$ then ε_p should be of $O(\nu^{1/2})$.

Figures 9 and 10 show the time history of ε_p for M_t=0.1 and 0.3, respectively. The constants $C_{\varepsilon p1}$=1.3 and M_{t0}=0.3 are chosen so that results from the model and the DNS agree with each other at St>7 for both cases. Although the result at St<7 for M_t=0.3 overestimates the DNS data, the difference between the two cases can be expressed by introducing the $R_{e\tau}$ part.

Next, we examine the pressure dilatation because it is significant for the development of pressure fluctuations. Although the pressure dilatation may be negligible in the K equation, it plays an important role in the $\langle p'^2\rangle$ equation. The model expression for the pressure dilatation is given by

$$\langle p'd'\rangle = -(1-C_{pd3}\chi_p)\left[C_{pd1}M_t^2\frac{D}{Dt}(\bar{\rho}K)+C_{pd2}\gamma\bar{\rho}M_t^2K\frac{\partial U_i}{\partial x_i}\right] \tag{11}$$

where

$$\chi_p = \langle p'^2 \rangle / (2\bar{\rho}^2 \bar{c}^2 K) \quad (12)$$

The nondimensional parameter χ_p is a normalized pressure variance that corresponds to the ratio of potential to kinetic energy for weak fluctuations. If we neglect χ_p and approximate $D(\bar{\rho}K)/Dt$ by $\bar{\rho}(P_K-\varepsilon)$ then the expression (11) is almost the same as the model derived by Sarkar (1992).

Figures 11 and 12 show the time history of the pressure dilatation for M_t=0.1 and 0.3, respectively. The model constants are set to C_{pd1}=1.3 and C_{pd3}=7 so that the overall agreement is good between the model and DNS results. The second term in the brackets in (11) vanishes for homogenous shear flows because of no mean-velocity divergence. If χ_p is negligible the pressure dilatation is proportional to $D(\bar{\rho}^2K^2)/Dt$. Substituting this form into (4) and assuming ε_p=0 gives $\langle p'^2 \rangle \sim \bar{\rho}^2 K^2$ that approximately holds for M_t=0.1 as shown in Fig. 3. The factor $1-C_{pd3}\chi_p$ represents the compressibility effect; that is, the growth rate of pressure dilatation is reduced for M_t=0.3 compared to the case of M_t=0.1. The part involving $D(\bar{\rho}K)/Dt$ represents nonequilibrium properties. For boundary layers and channel flows the value of $D(\bar{\rho}K)/Dt$ is negligible; the pressure dilatation is so small that it causes little pressure fluctuations. On the other hand, for homogenous shear flows and mixing layers $D(\bar{\rho}K)/Dt$ has some positive values; resulting negative pressure dilatation produces some amount of pressure fluctuations that contribute as the compressibility effect.

CONCLUSIONS

DNS of homogeneous shear flow was performed to investigate compressibility effects on turbulent energy growth. The normalized level of pressure fluctuations was shown to decrease as M_t increases. As is the case of mixing layers, this decrease causes the reduction in the pressure–strain term, changes the anisotropy of the Reynolds stress, and reduces the growth rate of turbulent kinetic energy. We examined the transport equation for the pressure variance to find that its dissipation term contributes to its reduction when M_t is high. The pressure-variance dissipation is closely related to the high-wavenumber part of the pressure-variance spectrum; if the spectrum is proportional to that for incompressible turbulent energy, the dissipation can be so large that it affects the evolution of the pressure variance. In the DNS the spectral form of the pressure variance is shown to depend on M_t.

The pressure–dilatation correlation is important in the transport equation for the pressure variance. The model expression for the pressure dilatation obtained from the TSDIA contains the material derivative of turbulent kinetic energy. This term represents nonequilibrium or unsteady properties of turbulent field and can explain the different compressibility effects between homogeneous shear flow and boundary layers.

REFERENCES

Bataille, F. and Bertoglio, J.-P., 1993, "Short and Long Term Behaviour of Weakly Compressible Turbulence," In FED-Vol. 151, *Transitional and Turbulent Compressible Flows*, ASME, pp. 139–145.

Bradshaw, P., 1996, "Turbulence Modeling with Application to Turbomachinery," *Prog. Aerospace Sci.*, Vol. 32, pp. 575–624.

Coleman, G. N., Kim, J., and Moser, R. D., 1995, "A Numerical Study of Turbulent Supersonic Isothermal-Wall Channel Flow," *J. Fluid Mech.*, Vol. 305, pp. 159–183.

Hamba, F., 1999, "Effects of Pressure Fluctuations on Turbulence Growth in Compressible Homogeneous Shear Flow," to be published in *Phys. Fluids*, Vol. 11, No. 6.

Hamba, F., and Blaisdell, G. A., 1997, "Towards Modeling Inhomogeneous Compressible Turbulence Using a Two-Scale Statistical Theory," *Phys. Fluids*, Vol. 9, pp. 2749–2768.

Huang, P. G., Coleman, G. N., and Bradshaw, P., 1995, "Compressible Turbulent Channel Flows: DNS Results and Modelling," *J. Fluid Mech.*, Vol. 305, pp. 185–218.

Lele, S. K., 1994, "Compressibility Effects on Turbulence," *Annu. Rev. Fluid Mech.*, Vol. 26, pp. 211–254.

Rubinstein, R., and Erlebacher, G., 1997, "Transport Coefficients in Weakly Compressible Turbulence," *Phys. Fluids*, Vol. 9, pp. 3037–3057.

Sarkar, S., 1992, "The Pressure–Dilatation Correlation in Compressible Flows," *Phys. Fluids* A, Vol. 4, pp. 2674–2682.

Sarkar, S., 1995, "The Stabilizing Effect of Compressibility in Turbulent Shear Flow," *J. Fluid Mech.*, Vol. 282, pp. 163–186.

Vreman, A. W., Sandham, N. D., and Luo, K. H., 1996, "Compressible Mixing Layer Growth Rate and Turbulence Characteristics," *J. Fluid Mech.*, Vol. 320, pp. 235–258.

Yoshizawa, A., 1992, "Statistical Analysis of Compressible Turbulent Shear Flows with Special Emphasis on Turbulence Modeling," *Phys. Rev.* A, Vol. 46, pp. 3292–3306.

Yoshizawa, A., 1995, "Simplified Statistical Approach to Complex Turbulent Flows and Ensemble-Mean Compressible Turbulence Modeling, *Phys. Fluids*, Vol. 7, pp. 3105–3117.

Yoshizawa, A., 1998, *Hydrodynamic and Magnetohydrodynamic Turbulent Flows, Modelling and Statistical Theory*, Kluwer, Dordrecht.